

Effects of ultraviolet treatment on the contact resistivity and electronic transport at the Ti/ZnO interfaces

Yow-Jon Lin, Chia-Lung Tsai, W.-R. Liu, W. F. Hsieh, C.-H. Hsu, Hou-Yen Tsao, Jian-An Chu, and Hsing-Cheng Chang

Citation: *Journal of Applied Physics* **106**, 013701 (2009); doi: 10.1063/1.3157201

View online: <http://dx.doi.org/10.1063/1.3157201>

View Table of Contents: <http://scitation.aip.org/content/aip/journal/jap/106/1?ver=pdfcov>

Published by the [AIP Publishing](#)

Articles you may be interested in

[Comparison of Ti Al Pt Au and Ti Au Ohmic contacts on n-type ZnCdO](#)

Appl. Phys. Lett. **88**, 012109 (2006); 10.1063/1.2161927

[Low-resistance ohmic contacts to p - Zn Mg O grown by pulsed-laser deposition](#)

Appl. Phys. Lett. **86**, 192103 (2005); 10.1063/1.1925309

[Carrier concentration dependence of Ti/Al/Pt/Au contact resistance on n-type ZnO](#)

Appl. Phys. Lett. **84**, 544 (2004); 10.1063/1.1644318

[Specific contact resistance of Ti/Al/Pt/Au ohmic contacts to phosphorus-doped ZnO thin films](#)

J. Vac. Sci. Technol. B **22**, 171 (2004); 10.1116/1.1641060

[Low-resistance Ti/Au ohmic contacts to Al-doped ZnO layers](#)

Appl. Phys. Lett. **77**, 1647 (2000); 10.1063/1.1308527



Re-register for Table of Content Alerts

Create a profile.



Sign up today!



Effects of ultraviolet treatment on the contact resistivity and electronic transport at the Ti/ZnO interfaces

Yow-Jon Lin,^{1,a)} Chia-Lung Tsai,² W.-R. Liu,^{3,4} W. F. Hsieh,³ C.-H. Hsu,^{3,4} Hou-Yen Tsao,¹ Jian-An Chu,¹ and Hsing-Cheng Chang⁵

¹*Institute of Photonics, National Changhua University of Education, Changhua 500, Taiwan*

²*Department of Physics, National Changhua University of Education, Changhua 500, Taiwan*

³*Department of Photonics and Institute of Electro-optical Engineering, National Chiao Tung University, Hsinchu 300, Taiwan*

⁴*Research Division, National Synchrotron Radiation Research Center, Hsinchu 300, Taiwan*

⁵*Department of Automatic Control Engineering, Feng Chia University, Taichung 407, Taiwan*

(Received 31 March 2009; accepted 26 May 2009; published online 1 July 2009)

We report on the effect of ultraviolet (UV) treatment on the specific contact resistance (ρ) and electronic transport at the Ti/ZnO interfaces. The experimental results show the same barrier height of Ti/ZnO samples without UV treatment as Ti/ZnO samples with UV treatment and the higher ρ of Ti/ZnO samples with UV treatment than Ti/ZnO samples without UV treatment, suggesting the barrier-height independence of ρ . Based on the thermionic-emission model and x-ray photoelectron spectroscopy results, we found that the induced decrease in the number of the hydroxides at the surface region of ZnO by UV treatment resulted in decreases in the electron concentration near the surface region and the excess current component related to tunneling, increasing in ρ of Ti/ZnO samples. © 2009 American Institute of Physics. [DOI: 10.1063/1.3157201]

I. INTRODUCTION

ZnO is a versatile material. ZnO has a direct band gap at room temperature with a large exciton binding energy and a strong cohesive energy. Its applications include antireflection coatings, transparent conducting electrodes, light-emitting diodes, flexible displays, and solar cells.^{1–8} The achievement of acceptable device characteristics relies heavily on developing low specific contact resistance (ρ) Ohmic metallization schemes.⁹ To produce low-resistance Ohmic contacts, a fairly high annealing temperature is required. However, thermal annealing at high temperature may cause surface roughening, surface decomposition, and spiky interfaces resulting in the deterioration of device performance and hence device reliability.^{10,11} To fabricate high-performance optoelectronic devices, low-resistance nonalloyed Ohmic contacts are essential. Treatment of the ZnO surface prior to any metal deposition has been used to decrease the contact resistivity.^{12,13} In the paper, we report on the effect of ultraviolet (UV) treatment on the contact resistivity of nonalloyed Ti Ohmic contacts to ZnO films grown by pulsed-laser deposition (PLD). The mechanisms of Ti Ohmic contacts to ZnO films with and without UV treatment were also investigated in this study. According to the experimental results, we found the same barrier height (ϕ_B) of Ti/ZnO samples without UV treatment as Ti/ZnO samples with UV treatment and the higher ρ of Ti/ZnO samples with UV treatment than Ti/ZnO samples without UV treatment, suggesting the barrier-height independence of ρ . Based on the thermionic-emission (TE) model and x-ray photoelectron spectroscopy (XPS) results, we found that the induced decrease in the number of the hydroxides at the surface region of ZnO by UV treatment

resulted in decreases in the electron concentration near the surface region and the excess current component related to tunneling, increasing ρ of Ti/ZnO samples.

II. EXPERIMENT PROCEDURE

The 600 nm ZnO film grown on a (0001) sapphire substrate by PLD is used in this study. In previous studies,^{14–20} undoped and doped ZnO films have been fabricated by PLD. A KrF excimer laser (wavelength of 248 nm) was employed and the beam was focused to produce an energy density of 5–7 J cm⁻² at 10 Hz repetition rate on a commercial hot pressed stoichiometric ZnO (99.999% purity) target. The films were deposited at a growth rate of 94.25 nm/hr at 550 °C substrate temperature and a base vacuum of 1.2 × 10⁻⁸ Torr. No oxygen gas flow was introduced during the process of growth. These grown samples were cleaned with chemical solutions of trichloroethylene, acetone, and methanol. Then, the samples were rinsed with deionized water and immediately blown dry with N₂. In our experiments, the ZnO sample was irradiated in air for 30 min by a UV light source (output power density of 810 μW/cm²) with emission centered at 254 nm. Next, Ti was used as the electrode and vacuum evaporated on top of the ZnO samples with and without UV treatment. Ti was deposited using the sputter coater. X-ray diffraction (XRD) was employed to identify crystalline phases. Using a Ne–Cu laser (the 248.6 nm line) as an excitation source, the photoluminescence (PL) band was observed for ZnO samples with and without UV treatment at room temperature. XPS was employed to examine the changes in the surface band bending of ZnO, chemical bonding states of ZnO, and the band bending in ZnO near the Ti/ZnO interface. In this study, the surface band bending was determined by location of the energy of the valence band maximum (VBM) in photoemission from the sample. XPS

^{a)}Author to whom correspondence should be addressed. Electronic mail: rzt2390@yahoo.com.tw.

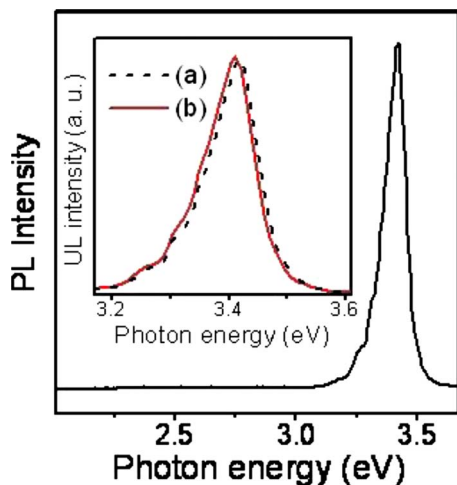


FIG. 1. (Color online) PL spectra of the ZnO films without UV treatment. Inset: UL spectra of the ZnO films (a) without and (b) with UV treatment.

system was equipped with monochromatic Al $K\alpha$ source. We took a Au $4f_{7/2}$ peak or a C $1s$ peak for energy reference purposes. All binding energies are measured relative to the Fermi level (E_F). ρ was measured using the circular transmission line method (CTLM)²¹ for Ti contact to ZnO with and without UV treatment at various temperatures between 300 to 400 K. The CTLM pattern was designed with a constant outer radius $r=100 \mu\text{m}$ and spacings of 2, 4, 8, 16, and $32 \mu\text{m}$. The current-voltage (I - V) characteristics of the Ti/ZnO samples were measured using a Keithley Model-4200 semiconductor characterization system.

III. EXPERIMENTAL RESULTS AND DISCUSSION

Figure 1 shows PL spectra of the ZnO film without UV treatment. One emission peak at room temperature was observed for ZnO samples. The peak at 3.42 eV is near band edge emission, the so called ultraviolet luminescence (UL). In Fig. 1, we do not find the green luminescence (peak position at $\sim 2.5 \text{ eV}$)²² related to the oxygen-vacancy-related emission.²³ The inset of Fig. 1 shows the UL spectra of the ZnO films with and without UV treatment. Compared with the ZnO films without UV treatment, we can see that the UL slightly shifted toward the low photon energy for ZnO films with UV treatment. An explanation for this will be given later. Figure 2 shows the XRD pattern of the ZnO film.¹⁹ Diffraction peaks appearing at about 34.4° and 30.9° correspond to those from ZnO (002) and $\text{Zn}(\text{OH})_2$ (100) planes.^{24,25} However, the intensity of (100) peak is very weak. These results shown in Figs. 1 and 2 provide direct evidence on the deposition of the good-quality ZnO film.

Figure 3 shows the I - V characteristics of the Ti/ZnO samples with and without UV treatment, measured between metal pads with gap spacing of $8 \mu\text{m}$. The I - V characteristics of the Ti/ZnO samples with and without UV treatment show linear behavior. It indicates that the Ohmic performance can be obtained for Ti/ZnO samples. Then, ρ was measured using the CTLM applied to a structure with gap spacing. The associated resistance as a function of gap spac-

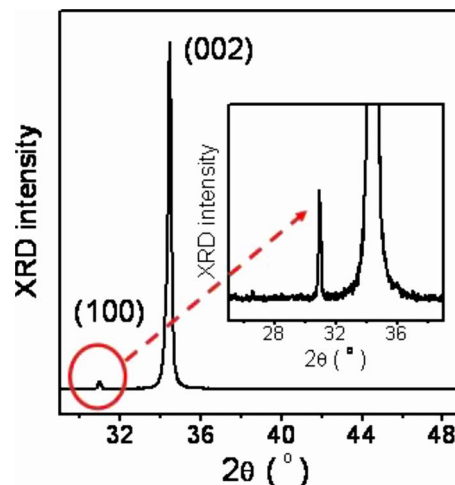


FIG. 2. (Color online) XRD 2θ scan of the ZnO films.

ing for Ti/ZnO samples can be obtained. ρ was determined to be 2.7×10^{-5} (4.1×10^{-6}) $\Omega \text{ cm}^2$ for Ti/ZnO samples with (without) UV treatment.

To study the formation mechanism of nonalloyed Ohmic contacts for Ti/ZnO samples with and without UV treatment, XPS was employed to determine the VBM position (E_v) of ZnO samples and the position ($E_{\text{ZnO}}^{\text{Zn } 3d}$) of Zn $3d$ core-level peak at the ZnO surfaces before Ti deposition. Figure 4 shows the Zn $3d$ core-level and valence-band spectra collected on a ZnO sample with or without UV treatment. E_v is determined by extrapolating two solid lines from the background and straight cutoff in the spectra.^{26,27} For ZnO samples without UV treatment, E_v was measured to be 3.52 eV and $E_{\text{ZnO}}^{\text{Zn } 3d}$ was observed at 10.96 eV, suggesting that the energy difference (E_{VC}) between $E_{\text{ZnO}}^{\text{Zn } 3d}$ and E_v is determined to be 7.44 eV, which agrees with the previously reported values of 7.3–7.5 eV.^{28–30} For ZnO samples with UV treatment, E_v was measured to be 2.50 eV and $E_{\text{ZnO}}^{\text{Zn } 3d}$ was observed at 10.24 eV, implying that E_{VC} is equal to 7.74 eV. The energy difference between E_{VC} of ZnO samples with and without UV treatment is attributed to the presence of dipole at the ZnO surface following UV treatment. In photoelectron

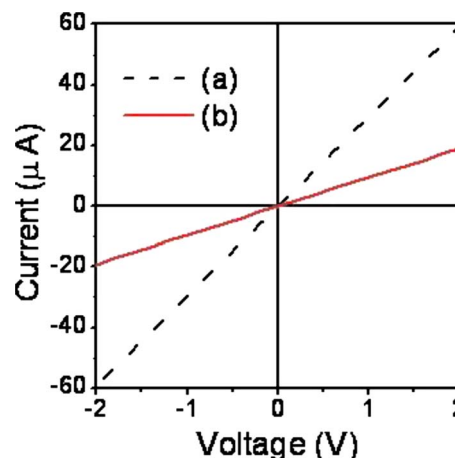


FIG. 3. (Color online) I - V characteristics of the Ti/ZnO samples (a) without and (b) with UV treatment measured between metal pads with gap spacing of $8 \mu\text{m}$.

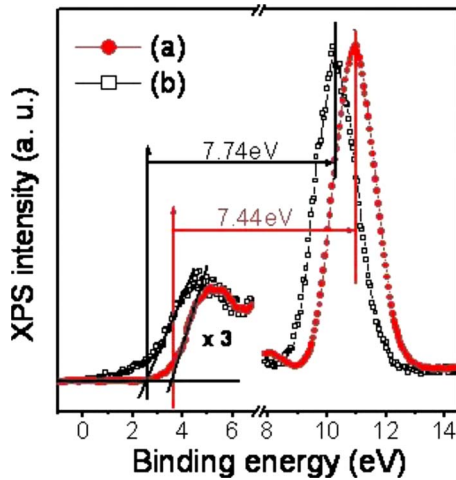


FIG. 4. (Color online) The left-hand figure presents the spectrum of the valence-band region and the right-hand spectrum shows the Zn 3d core-level spectra on the ZnO surfaces (a) without and (b) with UV treatment.

spectroscopy, the existence of a dipole at polar heterojunction can have a substantial influence on the measured binding energies of photoelectrons, depending on the origin of the collected photoelectrons being from below or above the heterojunction.³¹ Hong *et al.*²⁸ found the difference between VBM and Zn 3d level as 7.5 and 7.3 eV, respectively, before and after Ar⁺ ion cleaning. As a consequence, the measured binding energy can be smaller or larger, depending on the orientation of interface dipole. If the band gap energy (E_g) of ZnO was assumed to be 3.42 eV, E_F before UV treatment would be located at approximately 0.1 eV above the conduction band minimum (CBM) (that is, the formation of the downward band bending) and E_F following UV treatment would be located at approximately 0.92 eV below CBM (that is, the formation of the upward band bending).

Figure 5 shows the Zn 3d core-level XPS spectra at the Ti/ZnO interface with and without UV treatment. The peaks are determined by Gaussian fitting. ϕ_B at the Ti/ZnO interface was determined from the position ($E_{\text{Ti/ZnO}}^{\text{Zn } 3d}$) of Zn 3d

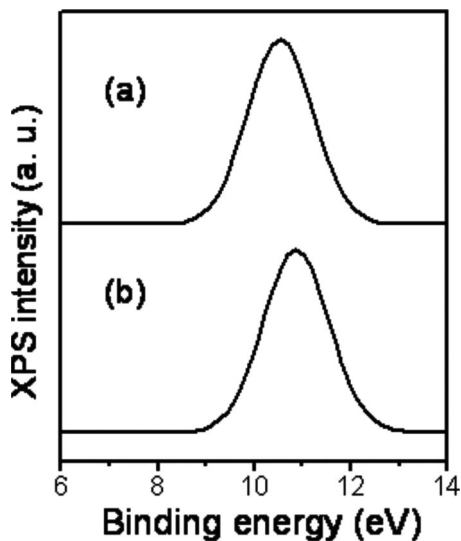


FIG. 5. Zn 3d core-level spectra at the Ti/ZnO interfaces (a) without and (b) with UV treatment.

core-level peak at the ZnO surfaces following Ti deposition and E_{VC} according to Eq. (1).³² Equation (1) is expressed as

$$\phi_B = E_g - (E_{\text{Ti/ZnO}}^{\text{Zn } 3d} - E_{VC}). \quad (1)$$

According to the result shown in Fig. 5, we find that $E_{\text{Ti/ZnO}}^{\text{Zn } 3d}$ without (with) UV treatment is located at 10.56 (10.86) eV. According to the result shown in Fig. 4, we find that E_{VC} without (with) UV treatment is equal to 7.44 (7.74) eV. Therefore, ϕ_B of the Ti/ZnO sample without (with) UV treatment was calculated to be 0.30 (0.30) eV. We find that ϕ_B of the Ti/ZnO sample without UV treatment is equal to ϕ_B of the Ti/ZnO sample with UV treatment, suggesting that ρ of the Ti/ZnO sample without UV treatment may be similar to ρ of the Ti/ZnO sample with UV treatment. However, ρ was determined to be $2.7 \times 10^{-5} \Omega \text{ cm}^2$ for Ti/ZnO samples with UV treatment which is higher than the determined value ($4.1 \times 10^{-6} \Omega \text{ cm}^2$) for Ti/ZnO samples without UV treatment. An explanation for this will be given latter. On the other hand, we use the TE theory to calculate the ϕ_B at the Ti/ZnO interface. According to the TE theory, the relationship between ρ and ϕ_B should be expressed as

$$\rho = \frac{k}{qA^*T} \exp\left(\frac{\phi_B}{kT}\right), \quad (2)$$

where A^* ($A^* = 32 \text{ A cm}^{-2} \text{ K}^{-2}$) (Ref. 19) is the effective Richardson constant of ZnO, q is the magnitude of the electron charge, k is the Boltzmann constant, and T is the absolute temperature. In Eq. (2), the contribution to current due to tunneling through the barrier is completely neglected. For the Ti/ZnO samples with and without UV treatment, ϕ_B values are 0.21 and 0.16 eV (based on the TE theory), respectively, which are not in agreement with the results from the direct measurement using XPS, of 0.3 and 0.3 eV, respectively. This experimental finding cannot be explained through Eq. (2). We propose that the origin of this result is tunneling through the barrier and ρ is related to the depletion-layer width (due to the higher ϕ_B determined by XPS measurement than the calculated value based on the TE theory). An explanation for this will be given later.

Figure 6 shows O 1s core-level spectra at the ZnO surfaces with and without UV treatment. Deconvolution of the O 1s core-level peak obtained via XPS studies of the ZnO surfaces without UV treatment revealed two peaks indicative of O–Zn and O–H (or O–OH) bonding,^{33–35} respectively. The peaks are determined by Gaussian fitting. The binding energy shown here has been scaled with respect to the position of the O–Zn bond peak. In Refs. 33–35, the binding energy of O–Zn (O–H or O–OH) bonds had been determined to be 531.3 (532.9) eV by XPS measurement. Therefore, the difference in the O–Zn bond and the O–H bond energies is determined to be 1.6 eV. The XPS result is in agreement with the XRD result [shown in Fig. 2]. Comparing the Ti/ZnO sample without UV treatment, we can see that the O–H bond peak in the XPS spectrum becomes a smaller fraction of the total O peak for the Ti/ZnO sample with UV treatment. First-principles calculations have provided evidence that H behaves as a shallow donor in ZnO and can be incorporated into the thin film via the formation of O–H bonds at the surface during growth.^{34,36} Cai *et al.*³⁷ suggested that the

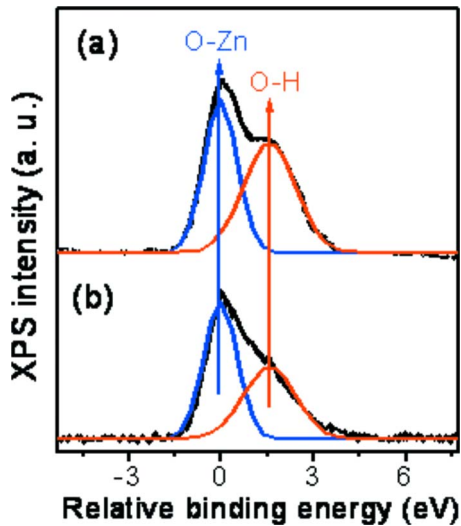


FIG. 6. (Color online) O $1s$ core-level spectra for ZnO samples (a) without and (b) with UV treatment.

incorporated hydrogen not only passivates most of the defects, but also introduces shallow donor states. Gu *et al.*³⁵ pointed out that the presence of the hydroxide constituent could lead to the formation of an accumulation layer having a high conductivity on the ZnO surface. Look *et al.*³⁸ found that the surface sheet carrier concentration increases with increasing the intensity of the O–H bond peak in the XPS spectrum. Mönch³⁹ pointed out that the current transport across metal-semiconductor contacts occurs by TE over the barrier for doping levels of the semiconductor up to approximately 10^{18} donors per cm^3 , while above this limit tunneling through the then narrower depletion layers dominates. This provides the evidence that a number of O–H bonds, acting as donors for electrons, were existed at the ZnO surfaces, resulting in the formation of low-resistance nonalloyed Ohmic contacts for Ti/ZnO samples without UV treatment. In addition, ρ was determined to be $2.7 \times 10^{-5} \Omega \text{ cm}^2$ for Ti/ZnO samples with UV treatment, which is higher than the determined value ($4.1 \times 10^{-6} \Omega \text{ cm}^2$) for Ti/ZnO samples without UV treatment. This is attributed to the presence of the wider depletion layer at the Ti/ZnO interface (due to the lower intensity of O–H bonds of Ti/ZnO samples with UV treatment than Ti/ZnO samples without UV treatment, as shown in Fig. 6), leading to a decrease in the probability of field emission. Consequently, we suggest that the tunneling plays an important role in the carrier transport across the barrier at the Ti/ZnO interface.

The measurement temperature dependence of ρ obtained on the basis of the TE model and CTLM data is shown in Fig. 7. It is worth noting that ρ obtained on the basis of CTLM data for Ti/ZnO samples with or without UV treatment is less sensitive to measurement temperature than that obtained on the basis of the TE model. Figures 7(b) and 7(c) show that the contacts exhibit almost constant ρ in the temperature range of 300–400 K. In addition, we find that ρ obtained on the basis of the TE model is higher than that obtained on the basis of CTLM data. These results show that the dominant mechanism of current transport is field emission.

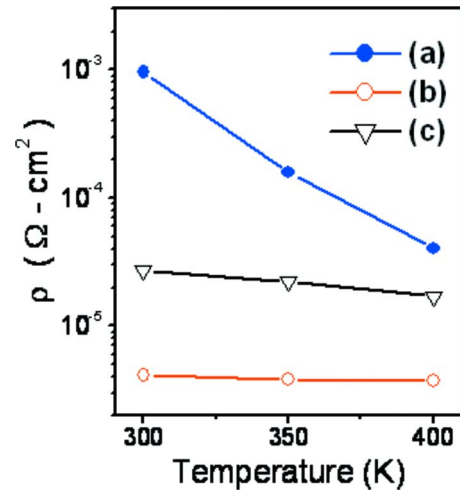


FIG. 7. (Color online) Variation in ρ with temperature: ρ [(a) Ti/ZnO samples ($\phi_B=0.3$ eV)] obtained on the basis of the TE model and ρ [Ti/ZnO samples (b) without and (c) with UV treatment] obtained on the basis of CTLM data.

The well-known equations for the electron concentration (n_3) and mobility (μ_3) in two-layer systems are expressed as^{38,40}

$$\mu_3 = \frac{n_1 d_1 \mu_1^2 + n_2 d_2 \mu_2^2}{n_1 d_1 \mu_1 + n_2 d_2 \mu_2}, \quad (3)$$

$$n_3 = \frac{(n_1 d_1 \mu_1 + n_2 d_2 \mu_2)^2}{(d_1 + d_2)(n_1 d_1 \mu_1^2 + n_2 d_2 \mu_2^2)}. \quad (4)$$

In Eqs. (3) and (4), n_1 and μ_1 represent the bulk, conduction-band electrons, and n_2 and μ_2 , the surface-layer electrons. d_1 is the bulk thickness and d_2 is the surface-layer thickness ($d_1 + d_2 = 600$ nm). However, the actual thickness of the surface layer is unknown. d_2 was assumed to be 4 nm in this study. According to the Van der Pauw–Hall measurements, we found that the electron concentration (n_3) and mobility (μ_3) of the ZnO films without UV treatment were calculated to be $4.3 \times 10^{17} \text{ cm}^{-3}$ and $12 \text{ cm}^2 \text{ V}^{-1} \text{ s}^{-1}$, respectively. According to the Van der Pauw–Hall measurements, we found that the electron concentration and mobility of the ZnO films with UV treatment were calculated to be $2.5 \times 10^{16} \text{ cm}^{-3}$ and $48 \text{ cm}^2 \text{ V}^{-1} \text{ s}^{-1}$, respectively. However, the actual n_1 and μ_1 of the bulk are difficult to obtain in this study. We assume that UV treatment may lead to the removal of the excess surface-layer electrons, meaning that n_1 (μ_1) can be assumed to be the electron concentration (mobility) of the ZnO films with UV treatment. Then, n_2 and μ_2 can be obtained from Eqs. (3) and (4). n_2 and μ_2 were estimated to be $5.3 \times 10^{20} \text{ cm}^{-3}$ and $1.12 \text{ cm}^2 \text{ V}^{-1} \text{ s}^{-1}$, respectively. Based on the XPS result shown in Fig. 6, the large portion of O–H bond peak comparing O–Zn peak still remained after UV treatment. However, we found that the surface-layer electron concentration was higher than 10^{19} cm^{-3} even for n_1 as low as 10^{15} cm^{-3} . Clearly, the higher surface-layer electron concentration than 10^{19} cm^{-3} could lead to the occurrence of carrier tunneling at the Ti/ZnO interface and an increase in E_g of ZnO determined by PL measurements. We deduce that the enlarged E_g of 3.42 eV and the detected shift in UL

spectra following UV treatment (shown in the inset of Fig. 1) are associated with a pronounced Burstein–Moss shift.⁴¹ According to the Burstein–Moss shift, the band gap widening for *n*-type semiconductors with a parabolic band is attributed to the free electron concentration. When the concentration of electrons in the conduction band exceeds the effective density of states in the conduction band of ZnO, the Fermi energy lies within the conduction band. The type of semiconductor is called degenerate *n*-type semiconductor.⁴² According to the XPS result shown in Fig. 4, we find that E_F before UV treatment is located at approximately 0.1 eV above CBM, suggesting the formation of the downward band bending and the occurrence of degeneration. These results demonstrate that the contact type conversion involves a decrease in the number of O–H bonds plus lowered tunneling due to UV treatment.

IV. CONCLUSIONS

The effect of UV treatment on the ρ and electronic transport at the Ti/ZnO interfaces has been researched in this study. We found that the tunneling plays an important role in the carrier transport across the barrier at the Ti/ZnO interface. The experimental results show the same ϕ_B of Ti/ZnO samples without UV treatment as Ti/ZnO samples with UV treatment and the higher ρ of Ti/ZnO samples with UV treatment than Ti/ZnO samples without UV treatment, suggesting the barrier-height independence of ρ . Therefore, we deduce the contribution to current due to tunneling through the barrier must be taken into account and ρ is related to the depletion-layer width. The XPS results also show the induced decrease in the number of the hydroxides at the surface region of ZnO by UV treatment. This provides the evidence that a decrease in the number of O–H bonds existed at the ZnO surfaces may result in a decrease in the electron concentration near the surface region, increasing the ρ of the Ti/ZnO samples.

ACKNOWLEDGMENTS

The authors acknowledge the support of the National Science Council of Taiwan (Contract No. 97-2628-M-018-001-MY3) in the form of grants.

¹C. Y. Chang, F. C. Tsao, C. J. Pan, G. C. Chi, H. T. Wang, J. J. Chen, F. Ren, D. P. Norton, and S. J. Pearton, *Appl. Phys. Lett.* **88**, 173503 (2006).

²M. C. Jeong, B. Y. Oh, M. H. Ham, and J. M. Myoung, *Appl. Phys. Lett.* **88**, 202105 (2006).

³S. H. K. Park, J. I. Lee, C. S. Hwang, and H. Y. Chu, *Jpn. J. Appl. Phys., Part 2* **44**, L242 (2005).

⁴Y. I. Alivov, J. E. V. Nostrand, D. C. Look, M. V. Chukichev, and B. M. Ataev, *Appl. Phys. Lett.* **83**, 2943 (2003).

⁵C. Yuen, S. F. Yu, S. P. Lau, and T. P. Chen, *Appl. Phys. Lett.* **86**, 241111 (2005).

⁶A. Tsukazaki, M. Kubota, A. Ohtomo, T. Onuma, K. Ohtani, H. Ohno, S. F. Chichibu, and M. Kawasaki, *Jpn. J. Appl. Phys., Part 2* **44**, L643 (2005).

⁷T. L. Yang, D. H. Zhang, J. Ma, H. L. Ma, and Y. Chen, *Thin Solid Films* **326**, 60 (1998).

⁸A. W. Ott and R. P. H. Chang, *Mater. Chem. Phys.* **58**, 132 (1999).

⁹A. A. Iliadis, R. D. Vispute, T. Venkatesan, and K. A. Jones, *Thin Solid Films* **420–421**, 478 (2002).

¹⁰Y. J. Lin and C. T. Lee, *Appl. Phys. Lett.* **77**, 3986 (2000).

¹¹H. K. Kim, S. H. Han, T. Y. Seong, and W. K. Choi, *Appl. Phys. Lett.* **77**, 1647 (2000).

¹²T. Akane, K. Sugioka, and K. Midorikawa, *J. Vac. Sci. Technol. B* **18**, 1406 (2000).

¹³J. M. Lee, K. K. Kim, S. J. Park, and W. K. Choi, *Appl. Phys. Lett.* **78**, 3842 (2001).

¹⁴W. R. Liu, W. F. Hsieh, C. H. Hsu, K. S. Liang, and F. S. S. Chien, *J. Cryst. Growth* **297**, 294 (2006).

¹⁵X. W. Sun and H. S. Kwok, *J. Appl. Phys.* **86**, 408 (1999).

¹⁶J. J. Chen, T. J. Anderson, S. Jang, F. Ren, Y. J. Li, H. S. Kim, B. P. Gila, D. P. Norton, and S. J. Pearton, *J. Electrochem. Soc.* **153**, G462 (2006).

¹⁷M. Brandt, H. Wenckstern, H. Schmidt, A. Rahm, G. Biehne, G. Benndorf, H. Hochmuth, M. Lorenz, C. Meinecke, T. Butz, and M. Grundmann, *J. Appl. Phys.* **104**, 013708 (2008).

¹⁸K. Ip, Y. W. H. Baik, D. P. Norton, S. J. Pearton, and F. Ren, *Appl. Phys. Lett.* **84**, 544 (2004).

¹⁹C. L. Tsai, Y. J. Lin, Y. M. Chin, W.-R. Liu, W. F. Hsieh, C.-H. Hsu, and J. A. Chu, *J. Phys. D: Appl. Phys.* **42**, 095108 (2009).

²⁰Y. J. Lin, S. S. Chang, H. C. Chang, and Y. C. Liu, *J. Phys. D: Appl. Phys.* **42**, 075308 (2009).

²¹H. S. Yang, Y. Li, D. P. Norton, K. Ip, S. J. Pearton, S. Jang, and F. Ren, *Appl. Phys. Lett.* **86**, 192103 (2005).

²²Ü. Özgür, Y. I. Alivov, C. Liu, A. Teke, M. A. Reshchikov, S. Doğan, V. Avrutin, S. J. Cho, and H. Morkoç, *J. Appl. Phys.* **98**, 041301 (2005).

²³Y. J. Lin, C. L. Tsai, Y. M. Lu, and C. J. Liu, *J. Appl. Phys.* **99**, 093501 (2006).

²⁴S. Zhao, Z. Ji, C. Wang, and J. Du, *Mater. Lett.* **61**, 897 (2007).

²⁵Z. Ji, S. Zhao, C. Wang, and K. Liu, *Mater. Sci. Eng., B* **117**, 63 (2005).

²⁶Y. J. Lin, F. M. Yang, C. Y. Huang, W. Y. Chou, J. Chang, and Y. C. Lien, *Appl. Phys. Lett.* **91**, 092127 (2007).

²⁷S. Y. Kim, J. M. Baik, H. K. Yu, and J. L. Lee, *J. Appl. Phys.* **98**, 093707 (2005).

²⁸S. K. Hong, T. Hanada, H. Makino, Y. Chen, H. J. Ko, A. Tanaka, H. Sasaki, and S. Sato, *Appl. Phys. Lett.* **78**, 3349 (2001).

²⁹M. Ruckh, D. Schmid, and H. W. Schock, *J. Appl. Phys.* **76**, 5945 (1994).

³⁰S. K. Hong, T. Hanada, H. Makino, H. J. Ko, Y. Chen, T. Yao, A. Tanaka, H. Sasaki, S. Sato, D. Imai, K. Araki, and M. Shinohara, *J. Vac. Sci. Technol. B* **19**, 1429 (2001).

³¹C. L. Wu, H. M. Lee, C. T. Kuo, S. Gwo, and C. H. Hsu, *Appl. Phys. Lett.* **91**, 042112 (2007).

³²J. R. Waldrop and R. W. Grant, *Appl. Phys. Lett.* **52**, 1794 (1988).

³³B. J. Coppa, C. C. Fulton, P. J. Hartlieb, R. F. Davis, B. J. Rodriguez, B. J. Shields, and R. J. Nemanich, *J. Appl. Phys.* **95**, 5856 (2004).

³⁴B. J. Coppa, C. C. Fulton, S. M. Kiesel, R. F. Davis, C. Pandarinath, J. E. Burnette, R. J. Nemanich, and D. J. Smith, *J. Appl. Phys.* **97**, 103517 (2005).

³⁵Q. L. Gu, C. K. Cheung, C. C. Ling, A. M. C. Ng, A. B. Djurišić, L. W. Lu, X. D. Chen, S. Fung, C. D. Beling, and H. C. Ong, *J. Appl. Phys.* **103**, 093706 (2008).

³⁶Ç. Kiliç and A. Zunger, *Appl. Phys. Lett.* **81**, 73 (2002).

³⁷P. F. Cai, J. B. You, X. W. Zhang, J. J. Dong, X. L. Yang, Z. G. Yin, and N. F. Chen, *J. Appl. Phys.* **105**, 083713 (2009).

³⁸D. C. Look, H. L. Mosbacher, Y. M. Strzhemechny, and L. J. Brillson, *Superlattices Microstruct.* **38**, 406 (2005).

³⁹W. Mönch, *J. Vac. Sci. Technol. B* **17**, 1867 (1999).

⁴⁰D. C. Look and R. J. Molnar, *Appl. Phys. Lett.* **70**, 3377 (1997).

⁴¹X. H. Zhou, Q. H. Hu, and Y. Fu, *J. Appl. Phys.* **104**, 063703 (2008).

⁴²D. A. Neamen, *Semiconductor Physics and Devices* (McGraw-Hill, Boston, 2003).